https://doi.org/10.20965/jaciii.2007.p0946

Paper:

The Design of Central Pattern Generators Based on the Matsuoka Oscillator to Generate Rhythmic Human-Like Movement for Biped Robots

Guang Lei Liu, Maki K. Habib, Keigo Watanabe, and Kiyotaka Izumi

Department of Advanced Systems Control Engineering, Graduate School of Science and Engineering, Saga University
1 Honjomachi, Saga 840-8502, Japan
liuguanglei@hotmail.com, {habib, watanabe, izumi}@me.saga-u.ac.jp

[Received March 19, 2007; accepted May 23, 2007]

We propose a controller based on a central pattern generator (CPG) network of mutually coupled Matsuoka nonlinear neural oscillators to generate rhythmic human-like movement for biped robots. The parameters of mutually inhibited and coupled Matsuoka oscillators and the necessary interconnection coupling coefficients within the CPG network directly influence the generation of the required rhythmic signals related to targeted motion. Our objective is to analyze the mutually coupled neuron models of Matsuoka oscillators to realize an efficient CPG design that leads to have dynamic, stable, sustained rhythmic movement with robust gaits for bipedal robots. We discuss the design of a CPG model with new interconnection coupling links and its inhibitation coefficients for a CPG-based controller. The new design was studied through interaction between simulated interconnection coupling dynamics with six links and a musculoskeletal model with the 6 degrees of freedom (DOFs) of a biped robot. We used the weighted outputs of mutually inhibited oscillators as torques to actuate joints. We verified the effectiveness of our proposal through simulation and compared the results to those of Taga's CPG model, confirming better, more efficient generation of stable rhythmic walking at different speeds and robustness in response to disturbances.

Keywords: central pattern generator (CPG), nonlinear neural oscillator, rhythmic movement, biped locomotion, biped robot.

1. Introduction

Challenges facing the development of autonomous biped robots include problems related to equilibrium and control strategies that must be solved to design efficient, stable rhythmic movement. Current locomotion control approaches are based mainly on trajectory plans that prescribe the desired state of movement as a function of time [1]. Most humanoids developed use the target zero moment point (ZMP) tracking algorithm for bipedal locomotion to describe system stability and to control a system by following a target ZMP trajectory [2]. While this control strategy is a simple, straightforward way to realize biped robots, it requires precise modeling and precise joint actuation with high joint control gain to achieve successful locomotion. We must understand how the human nervous system controls bipedal locomotion and how to model it with efficient controllers if we are to design humanoid robots with a human-like gait.

In efforts to understand robot locomotion control and to construct autonomous robots, robotics researchers have derived inspiration from biologically inspired control. Locomotion is a basic organic concept involving a nervous system dedicated for functionality of movement. Organic movement involves active interaction with the environment, rapid adaptability and stability toward environmental change, and robustness toward perturbations. From the viewpoint of neurobiology, human-like locomotion is hierarchically controlled at several levels of the central nervous system, i.e., the spinal cord, brainstem, and cerebral cortex [3]. Neurobiological studies have shown that rhythmic motor patterns are controlled by neural oscillators called central pattern generators (CPGs) [4]. Stable, adaptive walking results from interaction between musculoskeletal dynamics and the rhythmic CPG signals. CPGs most likely found in the spinal cord control low-level locomotion patterns such as walking, flying, crawling, and swimming in vertebrates [5, 6]. Evidence shows that animals have inherent rhythmic pattern generators within their neural circuitry [7]. CPGs have been studied in animals such as cats, and observations support the notion of human-CPGs. CPGs are biological neural networks that generate basic rhythmic movement in locomotion, such as walking, running, swimming, and flying. Rhythmic movements induce physical coordination [5], especially in higher vertebrates, for controlling posture and balance.

Nonlinear oscillators are systems of differential equations featuring such desirable features as robustness, independence from initial conditions, and synchronization. Several types of coupled nonlinear oscillators have been developed by Hopf, Rayleigh, Van del Pol, and Matsuoka to implement CPGs and generate required signals. Most CPGs for robot locomotion control covered in the literature are modeled as groups of coupled nonlinear differ-

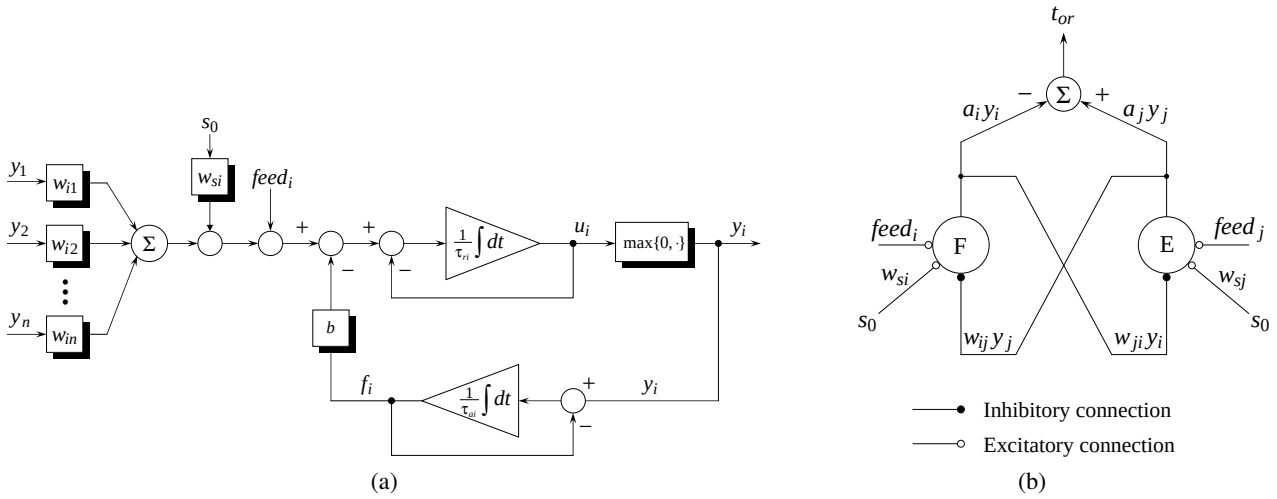

Fig. 1. (a) General Matsuoka neuron model; (b) One oscillator consisting of an extensor and a flexor.

ential equations, with flexible movement generated by entraining neural and mechanical dynamics in a dynamically changing environment. Matsuoka [8, 9] mathematically modeled the firing rate of two mutually inhibiting neurons for a neural oscillator, described by a set of differential equations. The Matsuoka oscillator is widely used to simulate biologically inspired movement and to generate rhythmic movement patterns for robots because the basic oscillator structure is simpler than that of other oscillators, e.g., the Van del Pol oscillator, because the Matsuoka oscillator has logical nonlinearity only in output, while the Van del Pol oscillator has quadratic state nonlinearity.

Interest is growing in biologically inspired control approaches for developing CPGs-based controllers to generate stable, efficient walking rhythm for robots with different locomotion, e.g., biped, quadruped, and hexapod [5, 10–12]. Such interest is reflected in the large numbers of studies, for example, on locomotion and swimming robots controlled by CPG controllers inspired by vertebrate locomotion. While many researchers have applied CPG-based concepts to walking robot control [10–20], controller parameters have mostly been tuned by trial and error.

We analyzed the internal Matsuoka oscillator model to find efficient structural design for a CPG-based controller with new coupling link interconnection and inhibition coefficients that generate dynamic, stable, sustained rhythmic movement with robust gaits for bipedal robots. We studied new design through interaction between simulated six-link interconnection coupling dynamics and the 6 degrees of freedom (DOF) musculoskeletal of a biped robot. We studied the effectiveness of our proposal through simulation, and compared results to those for Taga's CPG model, analyzing the generation of stable rhythmic walking, changes in walking speed, and response to disturbances.

2. Oscillator Neuron Model and Generic CPG Structure

The mathematical model of Matsuoka's nonlinear neural oscillator [8, 9] is introduced as a generic element into a CPG-based controller developed for biped robot locomotion.

2.1. Matsuoka Oscillator Neuron Model

Originally, Matsuoka's neural model [8, 9], consisted of two first-order coupled differential equations, one representing the membrane potential of the neuron and the other the degree of neuron fatigue:

$$\tau_{ri}\frac{du_i}{dt} = -u_i + \sum_{j=1}^{n} w_{ij}y_j + w_{s_i}s_0 - bf_i + feed_i \quad \ldots\ldots\ldots\ldots (1)$$

$$\tau_{ai}\frac{df_i}{dt} = -f_i + y_i \quad \ldots\ldots\ldots\ldots (2)$$

$$y_i(u_i) = \max\{0, u_i\} \quad \ldots\ldots\ldots\ldots (3)$$

where the output of the neuron is nonlinear in a logic function.

The mathematical neuron model has two state variables and constant parameters but their values must be selected appropriately. The first is inner state variable u_i, corresponding to the membrane potential of the neuron. The second state variable is f_i, representing the degree of adaptation or self-inhibition in the i-th neuron, b is the adaptation constant, and y_i is the output of the i-th neuron. Subscripts i, j denote the neuron number, τ_{ri} is the time constant specifying the rise time when step input is given. The frequency of output is roughly proportional to $1/\tau_{ri}$. τ_{ai} is the time constant specifying the adaptation time lag, w_{ij} denotes the inhibitory synaptic connection weight from the j-th neuron to the i-th neuron, $w_{ij} \leq 0$ for $i \neq j$, and $w_{ij} = 0$ for $i = j$. $\sum(w_{ij}y_j)$ represents the total input from neurons inside a neural network, s_0 is constant drive input, and w_{s_i} denotes a drive input connection

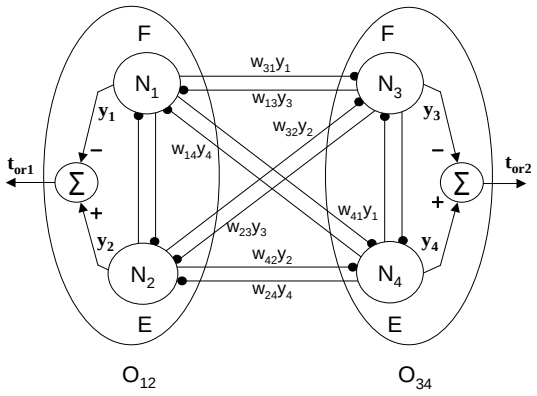

Fig. 2. Full and mutual inhibitory coupling between two Matsuoka oscillators.

Table 1. Neuron parameter setup within two Matsuoka oscillators in **Figs. 2** and **4**.

Parameter	τ_{ri}	τ_{ai}	w_{ij}	w_{s_i}	s_0	b	$feed_i$
N_1	1	12	—	2.0	1	2.5	0
N_2	1	12	—	2.0	1	2.5	0
N_3	1	12	—	1.5	1	2.5	0
N_4	1	12	—	1.5	1	2.5	0

weight. $feed_i$ is an input feedback sensor signal to the i-th neuron representing internal sensory information and interaction between the robot and its environment, and it is used mainly in a closed-loop CPG model or else is set to zero. Input $feed_i$ may be any number of inputs applied to the i-th neuron model, which may be either proprioceptive signals or signals from other neurons. Note that time constants τ_{ri} and τ_{ai} change frequency and that constant input s_0 changes amplitude. **Fig. 1(a)** shows the general Matsuoka neuron model described by Eqs. (1), (2), and (3).

Assuming that the Matsuoka oscillator consists of two neurons with four state variables, two variables represent the inner state of each neuron, u_i and u_j, and the other two state variables represent the degree of adaptation for each neuron, f_i and f_j. These neurons, linked reciprocally, alternately inhibit and excite each other to produce oscillation as output. Such activity accounts for the alternating and mutually inhibition of the flexor and extensor muscles at joints during walking. The extensor and flexor are physiologically driven based on the output of each neuron. Self-inhibition is governed by bf_i and bf_j connections and mutual inhibition by $w_{ij}y_j$ and $w_{ji}y_i$ connections. Oscillator output is $t_{or} = a_j y_j - a_i y_i$, representing the algebraic sum of the weighted output signal from each neuron, where a_i and a_j denote constant gains. t_{or} may be used as a motor command to drive a 1-DOF joint, where $t_{or} > 0$ implies extensor neuron activity, and $t_{or} < 0$ implies flexor neuron activity [14]. Conventionally, the output of oscillator t_{or} is used in the framework of feedforward control, where it is directly regarded as any manipulated quantity, such as torque, rate of angle, angle, etc., for each active joint in a robot. Here, the two neurons of each oscillator generate torques in opposite directions, i.e., the directions of flexor and extensor contraction. The algebraic sum of torques at each neural oscillator is proportional to the torque at the joint during biped walking.

Table 2. Weight coupling coefficients between the Matsuoka oscillators in **Fig. 2**.

		Oscillator 1		Oscillator 2	
		Neuron 1 (F)	Neuron 2 (E)	Neuron 3 (F)	Neuron 4 (E)
Oscillator 1	Neuron 1 (F)	—	−1.5	−2.0	−1.0
	Neuron 2 (E)	−1.5	—	−1.0	−1.0
Oscillator 2	Neuron 3 (F)	−2.0	−1.0	—	−2.0
	Neuron 4 (E)	−1.0	−1.0	−2.0	—

In a simplified Matsuoka oscillator model representing an extensor neuron or a flexor neuron (**Fig. 1(b)**), the neural oscillator causes attraction if provided with an input having a frequency similar to its natural frequency. τ_{ri}, τ_{ai}, b, and w_{ij} of both neurons must be optimized to achieve regular, sustainable oscillation generating stable rhythmic patterns. For a precise analysis of mathematical conditions generating oscillation, refer to [8] and [9].

2.2. Generic CPG Structure with Two Matsuoka Oscillators

The biological literature describes CPG network behavior but not its design. The CPG models biological rhythm represented using neural oscillators. Basically, coupled adaptive oscillators are used in CPG network construction to produce a periodic signal, particularly in a simple network based on inhibitory connections that enable reasonably predictable neural CPG design.

2.2.1. Full and Mutual Coupling Between Neuron Outputs of Two Matsuoka Oscillators

Extensor and flexor neuron output within one Matsuoka oscillator O_{12} consists of neurons 1 and 2, i.e., y_1 and y_2, considered as excitatory or inhibitory input to each extensor and flexor neuron in a second Matsuoka oscillator O_{34}, which consists of neurons 3 and 4 (**Fig. 2**). Similarly, extensor and flexor neuron output in the second Matsuoka oscillator O_{34}, which consists of neurons 3 and 4, i.e., y_3 and y_4, are considered as excitatory or inhibitory input to each extensor and flexor neuron in the first Matsuoka oscillator O_{12}, which consists of neurons 1 and 2.

Consider a case in which neuron outputs of two Matsuoka oscillators O_{12} and O_{34} are fully and mutually coupled through inhibition coupling coefficients, while key

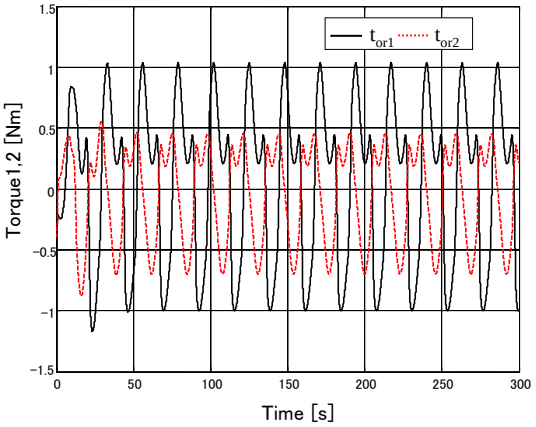

Fig. 3. Output response in full and mutual inhibitory coupling between two Matsuoka oscillators.

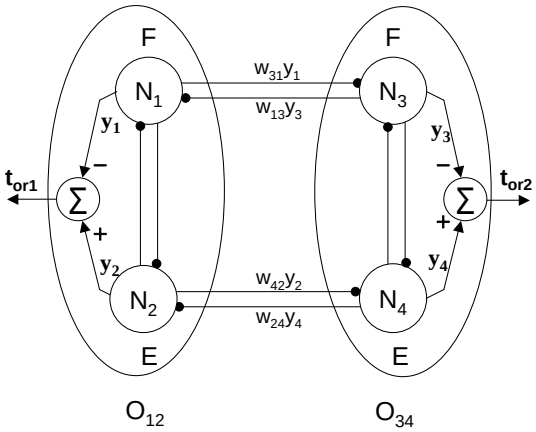

Fig. 4. Identical and mutual inhibitory coupling between two Matsuoka oscillators.

Table 3. Weight coupling coefficients between two Matsuoka oscillators in **Fig. 4**.

		Oscillator 1		Oscillator 2	
		Neuron 1 (F)	Neuron 2 (E)	Neuron 3 (F)	Neuron 4 (E)
Oscillator 1	Neuron 1 (F)	—	−1.5	−1.0	0.0
	Neuron 2 (E)	−1.5	—	0.0	−1.0
Oscillator 2	Neuron 3 (F)	−1.0	0.0	—	−2.0
	Neuron 4 (E)	0.0	−1.0	−2.0	—

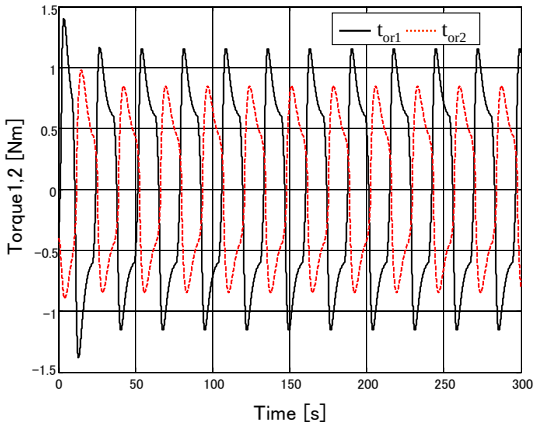

Fig. 5. Output response in identical and mutual inhibitory coupling between two Matsuoka oscillators.

parameters are set to ensure oscillatory conditions for each neuron (**Tables 1** and **2**). The simulation result is shown in **Fig. 3**.

2.2.2. Identical and Inhibitory Mutual Coupling Between Neuron Outputs of Two Matsuoka Oscillators

In another important and particular case, a generic CPG connection is obtained by having only mutual and identical inhibitory connections between the two oscillators, i.e., extensor neuron output from each oscillator is to be come inhibitory input to extensor neurons at other oscillators and vice versa. A similar connection is made for flexor neuron output at both oscillator (**Fig. 4**). Here, connection weight coefficients w_{13}, w_{24}, w_{31}, and w_{42} are negative and their values are assigned as shown in **Table 3**. The simulation result is shown in **Fig. 5**. Results show that output response (t_{or2}) of O_{34} is half a cycle behind output response (t_{or1}) of O_{12}. Such a generic CPG structure represents the cyclic hip movement of a biped robot suitably.

3. Biped Robot Model and CPG-Based Controller

In the CPG-based controller we developed, interaction is required among a high-level activity coordinator (nervous system), the controller, the robot, and the environment to fulfill tasks involving the generation of stable human-like motion for biped robots. Our goal is to test the developed CPG controller through simulation, so the robot requires a mathematical model. For this purpose, we modeled the biped robot with a musculoskeletal system [10], and mathematically formulated its dynamic equations of motion using the Newton-Euler method. Robot model walking results from torques generated via the CPG controller as motor commands and acting at each robot joint. The CPG controller continuously updates motor commands via feedback signals to establish a closed loop enabling real-time adaptation of the walking gait. The high-level activity coordinator sets and activates rhythmic neural movement based on external and internal sensory information.

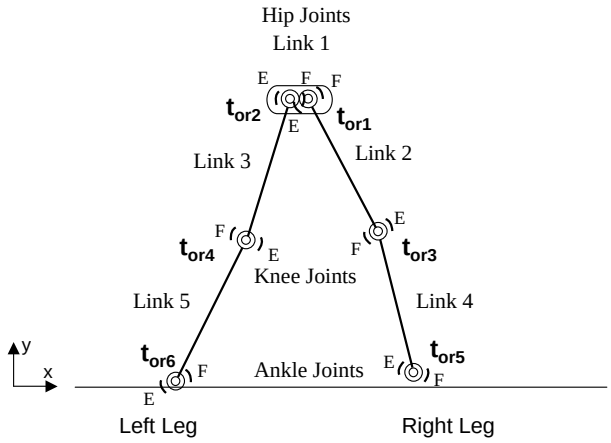

Fig. 6. Five-link biped robot model.

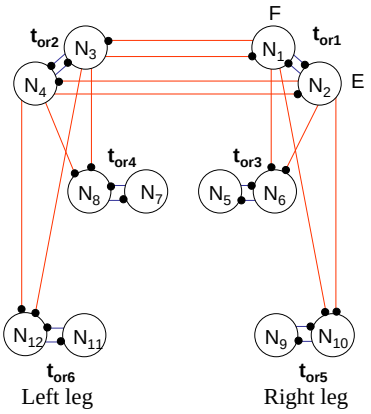

Fig. 7. One-rank CPG network of biped model.

3.1. Bipedal Musculoskeletal Model

The simple simulated bipedal musculoskeletal model (**Fig. 6**) considered here has six joints and two identical legs, each with three DOFs corresponding to the hip, knee, and ankle. Each leg consists of a thigh (links 2 and 3) and shank (links 4 and 5). In the dynamic bipedal musculoskeletal model, links are uniformly rectangular with a center of mass. A point mass is used to represent the remainder, described by link 1 at the hip. Both legs are integrated at link 1 while ensuring suitable detachment. Joints 1 and 2 are for the hips, Joints 3 and 4 for the knees, and Joints 5 and 6 for the ankles. Due to low inertia, the foot point has been considered dynamics during the support phase, and contact with the ground is represented by a two-dimensional spring and damper. Vertical and horizontal ground reaction are modeled and calculated while the feet touch the ground. A slippage model uses a condition that manages the relationship between reactive force and the static friction coefficient of the ground. The described model moves within the sagittal plane, and torques acting at joints to realize walking are assumed to be generated by the CPG controller.

3.2. Mathematical Model Movement Formulation

Using the Newton-Euler dynamic formulation, we derive general equations of motion for the bipedal musculoskeletal model as follows [14]:

$$\ddot{\boldsymbol{x}} = P(\boldsymbol{x})F + Q(\boldsymbol{x},\dot{\boldsymbol{x}},T_r(\boldsymbol{y}),F_g(\boldsymbol{x},\dot{\boldsymbol{x}})) \quad \ldots\ldots \quad (4)$$

where the $\boldsymbol{x} \in \Re^{14}$ vector of inertial positions of 5 links and inertial angles of 4 links; $P \in \Re^{14\times 8}$ matrix; $F \in \Re^8$ vector of constraint forces; $Q \in \Re^{14}$ vector; $T_r \in \Re^6$ vector of torques; $F_g \in \Re^4$ vector of forces on the ankle based on the terrain state; and $\boldsymbol{y} \in \Re^{12}$ vector of CPG controller output.

Equations of kinematic constraints are formulated from the model, and acceleration is obtained by differentiating these equations twice over time. The resulting equations are written compactly as follows:

$$C(\boldsymbol{x})\ddot{\boldsymbol{x}} = D(\boldsymbol{x},\dot{\boldsymbol{x}}). \quad \ldots\ldots\ldots\ldots \quad (5)$$

Constraint forces are obtained by substituting Eq. (4) into Eq. (5), and to get required acceleration without using constraint force, the resulting equation of force is substituted into Eq. (4). The compact form of acceleration equations representing bipedal musculoskeletal movement are as follows:

$$\begin{aligned}\ddot{\boldsymbol{x}} = {} & P(\boldsymbol{x})[C(\boldsymbol{x})P(\boldsymbol{x})]^{-1}[D(\boldsymbol{x},\dot{\boldsymbol{x}}) \\ & - C(\boldsymbol{x})Q(\boldsymbol{x},\dot{\boldsymbol{x}},T_r(\boldsymbol{y}),F_g(\boldsymbol{x},\dot{\boldsymbol{x}}))] \\ & + Q(\boldsymbol{x},\dot{\boldsymbol{x}},T_r(\boldsymbol{y}),F_g(\boldsymbol{x},\dot{\boldsymbol{x}})). \quad \ldots\ldots \quad (6)\end{aligned}$$

To solve movement equations, $\boldsymbol{y}$ values are provided as CPG output proportional to torque. The feedback signal from the bipedal robot to the CPG is represented by joint locations and velocity of different moving parts of the body and contact with the environment.

3.3. Biology-Inspired Controller

Six Matsuoka oscillators, i.e., 12 Matsuoka neuron models, are used to build the CPG-based controller for the bipedal robot, i.e., two oscillators for left and right hips and one oscillator for each knee and ankle (**Fig. 7**) [10]. Odd-numbered neurons, i.e., N_i, $i = 1,2,\ldots,12$, represent the flexor (F) and even-numbered neurons extensor (E), and t_{or1} to t_{or6} represent output torque from oscillators. The two hip oscillators are configured to have identical and mutual inhibitory connections. The inhibitory connection between hip oscillators produces alternate excitation for alternation between leg movement. Parameters for each neuron model and interconnection coupling coefficients between oscillators are tuned experimentally to generate a consistent pattern that yields human biped movement. The feedback signal from the bipedal robot to the CPG is represented by inertial joint locations and the velocity of different moving parts of the robot and contact with the environment. Feedback sensory information for a physical biped robot is sensed through internal and external sensors.

Interconnection coupling links between neural oscillators have been selected to produce stable and rhythmic relative phases at joints on either side of the biped robot. **Fig. 8** shows new coupling in which the hip oscillator flexor and extensor inhibit knee and ankle oscillator ex-

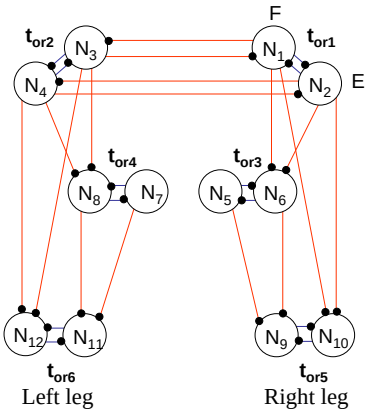

Fig. 8. Two-rank CPG network of biped model.

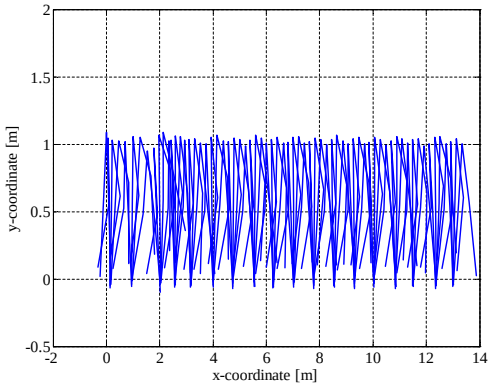

Fig. 9. Walking trajectory of Taga model with $s_0 = 5.5$ during 10 s simulation.

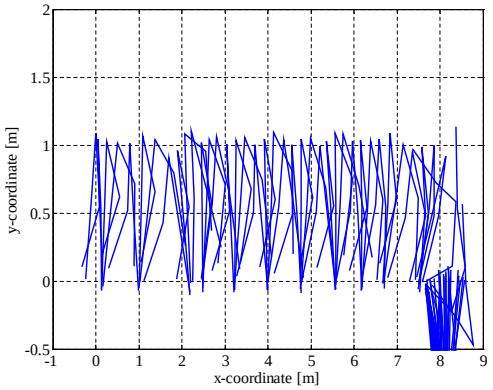

Fig. 10. Walking trajectory of Taga model with $s_0 = 6.0$ during 10 s simulation.

tensor neurons. The flexor and extensor of both knee oscillators were chosen to inhibit ankle flexor neurons. The new coupling links are expected to enable the CPG-based controller to generate better, stabler, rhythmic, and alternate relative phases for each side of the robot while enhancing robot response to external perturbations more than the model in **Fig. 7**.

4. Simulation and Results

4.1. Simulation

We simulated the three main components of the biped robot using MATLAB, as follows:

1. Vertical and horizontal ground contact are continuously calculated while any one or both of the bipedal ankles contact the ground. Ground contact was simulated using two-dimensional springs and dampers.

2. The CPG-based controller receives inputs as feedback signals from both ground contact and inertial locations and velocities from the musculoskeletal model. Using Eqs. (1), (2), and (3) and feedback signals together with assigned coupling coefficients, each of the Matsuoka oscillators generates an output weighted with a gain constant to yield the instantaneous torque required to actuate the joint instantaneously.

3. We simulated musculoskeletal dynamics using Eq. (6). This part of the simulation receives generated torque through the CPG-based controller and ground contact. Its outputs are a set of inertial locations and velocities for hips and ankles and for centers of thigh and shank links and a set of angles and angular velocities for center locations of thigh and shank links.

The three components above were implemented and execution synchronized every 0.001 s.

4.2. Conventional Coupling Among Joints and Parameter Settings

We first tested the simulator using the CPG-based controller (**Fig. 7**) with the same initial parameters as used by Taga et al. [10]. This model was tested with different settings for external drive input s_0. Results showed that walking stability becomes very critical when this parameter value was changed even slightly (**Figs. 9** and **10**) where s_0 was set to 5.5 and 6.0. **Fig. 11** shows the output torque response of joints 2, 4, and 6 (left leg) when s_0 = 6.0 and highlights events causing the robot to collapse when the torque response of joints 2, 4, and 6 fail to generate the required rhythmic movement.

Another factor was considered to analyze the stability of the Taga model while it is subjected to an external force of 200 N horizontally at the center of mass between hip joints and for different duration when s_0 is set first to 5.5. **Fig. 12** shows that the model maintains a stable walking trajectory after being subjected to 200 N for 200 ms at the beginning of 3 s after simulation starts. The Taga model cannot continue walking after being subjected to 200 N for 400 ms at the beginning of 3 s starting simulation when s_0 was set to 5.5.

Simulation results also show that the Taga model cannot keep a stable walking trajectory when s_0 is set to 6.5 while it is subjected to an external force of 200 N horizon-

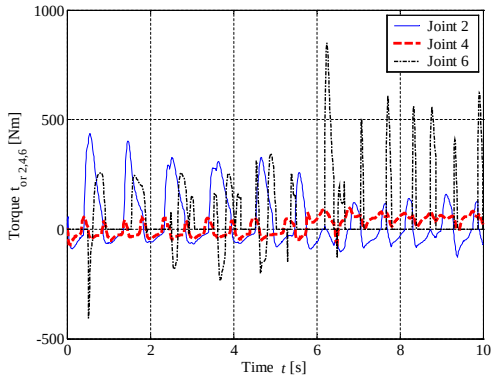

Fig. 11. Output torque response of joints 2, 4, and 6 (left leg) using Taga model with $s_0 = 6.0$ during 10 s simulation.

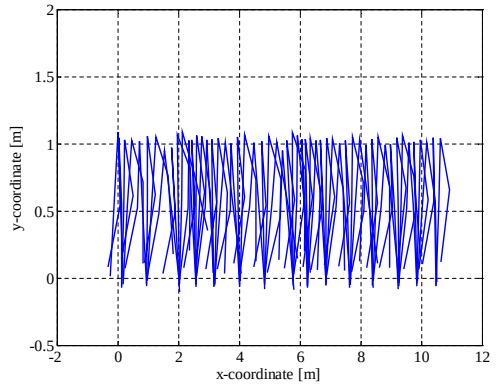

Fig. 12. Walking trajectory with external force applied horizontally to the center of mass between hip joints for 200 ms and with $s_0 = 5.5$ for 8 s simulation with Taga model.

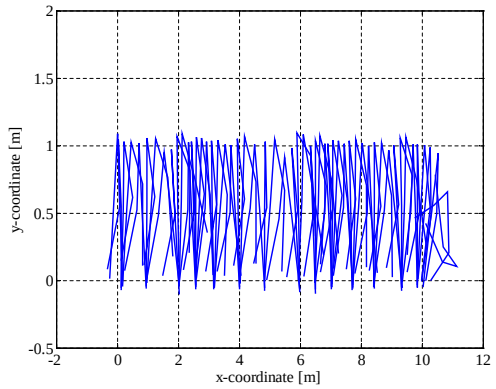

Fig. 13. Walking trajectory with external force applied horizontally to the center of mass between hip joints for 400 ms and with $s_0 = 5.5$ for 8 s simulation with Taga model.

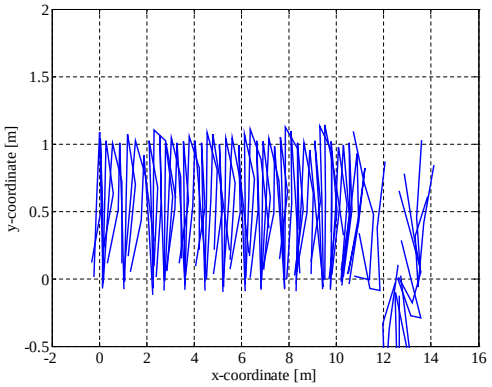

Fig. 14. Walking trajectory with external force applied horizontally to the center of mass between hip joints for 100 ms and with $s_0 = 6.5$ for 8 s simulation with Taga model.

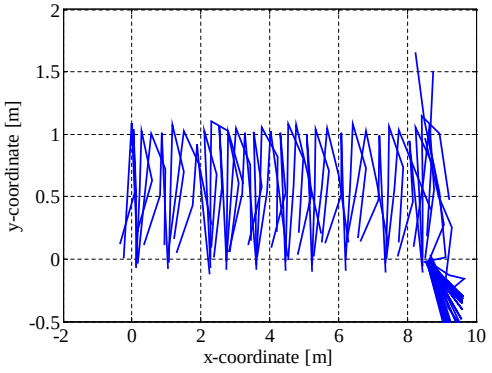

Fig. 15. Walking trajectory with external force applied horizontally to the center of mass between hip joints for 400 ms and with $s_0 = 6.5$ for 8 s simulation with Taga model.

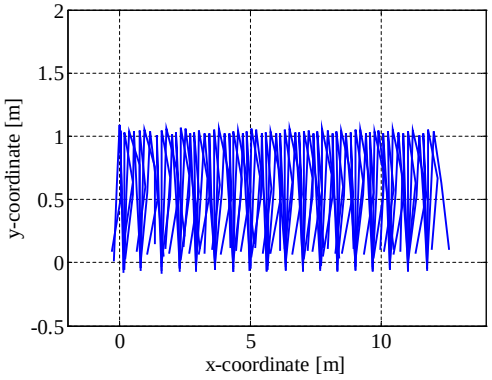

Fig. 16. Walking trajectory of developed model with $s_0 = 5.5$ during 10 s simulation.

tally at the center of mass between hip joints and for any duration. The model collapsed after being subjected to the above force for 100 ms (**Fig. 14**) and 400 ms (**Fig. 15**).

4.3. New Coupling Among Joints and Parameter Settings

Second, we tested the simulator using our CPG-based controller (**Fig. 8**), using the same initial parameters [10], together with new weight coupling coefficients (all -0.5) for the new connections from the knee extensor and flexor to the ankle flexor. Taga's initial setting was used to facilitate the comparison between Taga's model and ours.

Similar tests were conducted (**Figs. 16** and **17**) with 5.5 and 6.0 assigned to s_0. **Fig. 18** shows the output torque response of joints 2, 4, and 6 (left leg) using our model with new connections when $s_0 = 6.0$. **Figs. 19–22** show our model's robustness when tested under external perturbations. Our CPG-based model has clear advantages in maintaining sustained, stable walking trajectories at dif-

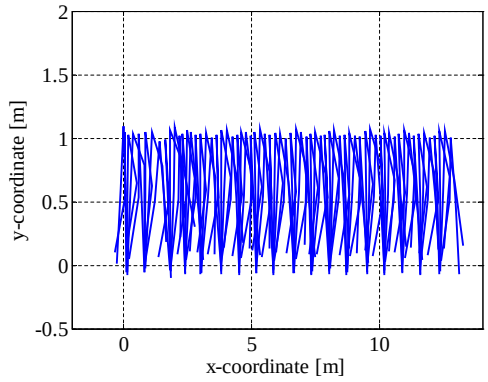

Fig. 17. Walking trajectory of developed model with $s_0 = 6.0$ during 10 s simulation.

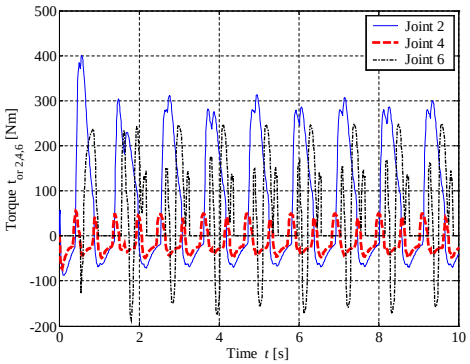

Fig. 18. Output torque response of joints 2, 4, and 6 (left leg) using the developed model with new connections $s_0 = 6.0$ during 10 s simulation.

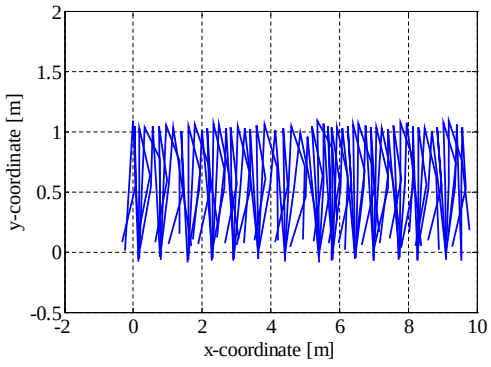

Fig. 19. Walking trajectory with external force applied horizontally to the center of mass between hip joints for 200 ms and with $s_0 = 5.5$ for 8 s simulation with the new model.

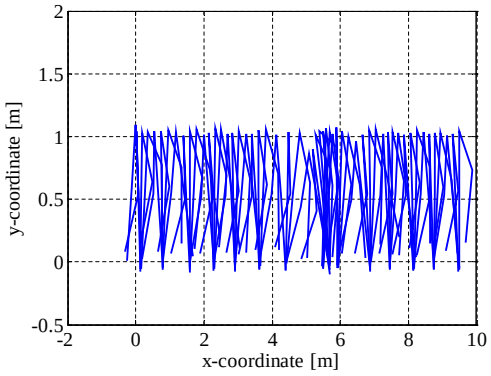

Fig. 20. Walking trajectory with external force applied horizontally to the center of mass between hip joints for 400 ms and with $s_0 = 5.5$ for 8 s simulation with the new model.

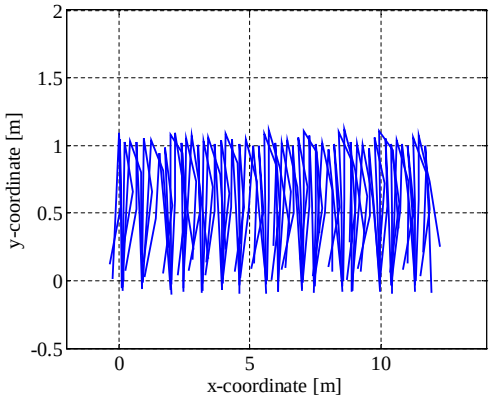

Fig. 21. Walking trajectory with external force applied horizontally to the center of mass between hip joints for 100 ms and with $s_0 = 6.5$ for 8 s simulation with the new model.

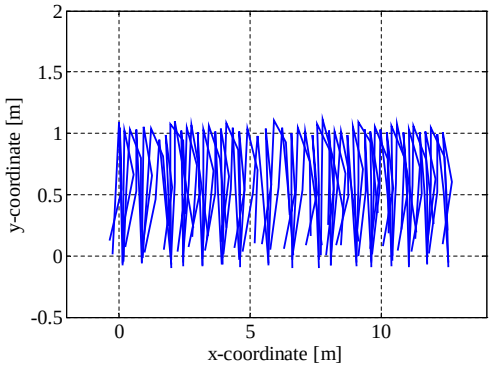

Fig. 22. Walking trajectory with external force applied horizontally to the center of mass between hip joints for 400 ms and with $s_0 = 6.5$ for 8 s simulation with the new model.

ferent walking speeds while responding robustly to external perturbations.

Test and analysis results are summarized in **Tables 4–7** to direct compare Taga's and our CPG model. ◯ denotes stable and × unstable locomotion. t_f denotes the time when the model fell and x_f denotes total walking distance at t_f. Final results clearly show the advantages of our approach.

5. Conclusions

We have proposed CPG-based control consisting of a network of mutually inhibited and coupled Matsuoka oscillators with new interconnections for generating rhythmic signals that lead to dynamic, stable movement for biped robots. Results of simulation experiments have shown that interconnection coupling links newly added to the CPG with its inhibitation coefficients ensured the gen-

Table 4. Status of walking trajectory with different s_0 during 10 s simulation.

	External drive input (s_0)				
	5.0	5.5	6.0	6.5	7.0
Taga et al.	× t_f = 3.9 s x_f = 5.2 m	○	× t_f = 6.0 s x_f = 8.8 m	○	× t_f = 2.8 s x_f = 5.3 m
Proposal	× t_f = 4.8 s x_f = 5.6 m	○	○	× t_f = 9.8 s x_f = 14.2 m	× t_f = 7.9 s x_f = 12.7 m

○ Stable locomotion; × Unstable locomotion

Table 5. Status of walking trajectory with different s_0 with external force of 200 N applied for 100 ms.

	External drive input (s_0)				
	5.0	5.5	6.0	6.5	7.0
Taga et al.	× t_f = 3.9 s x_f = 5.3 m	○	× t_f = 4.8 s x_f = 6.8 m	× t_f = 6.6 s x_f = 11.2 m	× t_f = 3.3 s x_f = 5.2 m
Proposal	× t_f = 4.8 s x_f = 5.9 m	○	○	○	○

○ Stable locomotion; × Unstable locomotion

Table 6. Status of walking trajectory when $s_0 = 5.5$ with external force of 200 N applied for different durations.

	Duration of external force [s]			
	0.1	0.2	0.3	0.4
Taga et al.	○	○	○	× t_f = 7.8 s x_f = 10.8 m
Proposal	○	○	○	○

○ Stable locomotion; × Unstable locomotion

Table 7. Status of walking trajectory when $s_0 = 6.5$ with external force of 200 N applied for different durations.

	Duration of external force [s]			
	0.1	0.2	0.3	0.4
Taga et al.	× t_f = 6.6 s x_f = 11.2 m	× t_f = 5.7 m x_f = 10.1 m	× t_f = 5.5 s x_f = 9.9 m	× t_f = 5.4 s x_f = 9.7 m
Proposal	○	○	○	○

○ Stable locomotion; × Unstable locomotion

eration of dynamic, stable, sustained rhythmic human like movement with robust gaits for bipedal robots at different walking speeds. Results also show that the CPG-based controller with new interconnections robustly recognized external perturbations and undertook actions appropriate for sustaining stable walking. No systematic design principle currently determines oscillator parameter values or efficiently assigns weight coupling coefficients between oscillators. Our next work is thus to focus on applying suitable learning optimizing the parameters of each neural oscillator toward reconfiguring the coupling mechanism in real time.

References:

[1] K. Hirai, M. Hirose, Y. Haikawa, and T. Takenaka, "The development of Honda humanoid robot," in Proc. of the Int. Conf. on Robotics and Automation (ICRA'98), Vol.2, pp. 1321-1326, 1998.

[2] M. Vukobratovic, B. Borovac, D. Surla, and D. Stokic, "Biped Locomotion: Dynamics Stability, Control and Application," New York, NY: Springer-Verlag, 1990.

[3] S. F. Giszter, K. A. Moxon, I. A. Rybak, and J. K. Chapin, "Neurobiological and neurorobotic approaches to control architectures for a humanoid motor system," J. of Robotics and Autonomous System, Vol.37, No.2-3, pp. 219-235, 2001.

[4] S. Grillner, P. Wallen, L. Brodin, and A. Lansner, "Neuronal network generating locomotor behavior in lamprey: Circuitry, transmitters, membrane properties, and simulation," Annual Review of Neuroscience, Vol.14, pp. 169-199, 1991.

[5] Delcomyn, "Neural basis of rhythmic behavior in animals," J. of Science, Vol.210, pp. 492-498, 1980.

[6] E. Marder and R. L. Calabrese, "Principles of rhythmic motor pattern generation," Physiological Review, Vol.76, pp. 687-717, 1996.

[7] A. H. Cohen, "Control principle for locomotion - looking toward biology," in Proc. of the 2nd Int. Symposium on Adaptive Motion of Animals and Machines, TuP-K-1, 2003.

[8] K. Matsuoka, "Sustained oscillations generated by mutually inhibiting neurons with adaptation," J. of Biological Cybernetics, Vol.52, pp. 367-376, 1985.

[9] K. Matsuoka, "Mechanisms of frequency and pattern control in the neural rhythm generators," J. of Biological Cybernetics, Vol.56, pp. 345-353, 1987.

[10] G. Taga, Y. Yamaguchi, and H. Shimizu, "Self-organized control of bipedal locomotion by neural oscillators in unpredictable environment," J. of Biological Cybernetics, Vol.65, pp. 147-159, 1991.

[11] Y. Nakamura, M. Sato, and S. Ishii, "Reinforcement learning for biped robot," in Proc. of the 2nd Int. Symposium on Adaptive Motion of Animals and Machines, Kyoto, March 4-8, 2003.

[12] T. Ishii, S. Masakado, and K. Ishii, "Locomotion of a quadruped robot using CPG," in Proc. of IJCNN'04, 2004.

[13] A. Fujii, A. Ishiguro, and P. E. Hotz, "Real-time action selection of a biped robot using polymorphic CPG circuits," J. of Robotics Society of Japan, Vol.22, No.4, pp. 478-484, 2004.

[14] J. J. Hu, M. M. William, and G. A. Pratt, "Bipedal locomotion control with rhythmic oscillators," in Proc. of the Int. Conf. on Intelligent Robots and Systems, pp. 1475-1481, 1999.

[15] M. Williamson, "Neural control of rhythmic arm movements," Neural Networks, Vol.11, pp. 1379-1394, 1988.

[16] M. Sugisaka, K. Imamura, K. Tokuda, and M. Masuda, "A new artificial life body: Biologically inspired dynamic bipedal humanoid robots," Artificial Life and Robotics, Vol.8, pp. 1-4, 2004.

[17] L. Righetti and A. J. Ijspeert, "Programmable central pattern generators: An application to biped locomotion control," in Proc. of the 2006 IEEE Int. Conf. on Robotics and Automation, pp. 1585-1590, 2006.

[18] Y. Fukuoka and H. Kimura, "Biologically inspired adaptive dynamic walking of a quadruped on irregular terrain," J. of Robotics Society of Japan, Vol.21, No.5, pp. 569-580, 2003.

[19] J. Nakanishi, J. Morimoto, G. Endo, G. Cheng, S. Schaal, and M, Kawato, "Learning from demonstration and adaptation of biped locomotion," J. of Robotics and Autonomous Systems, Vol.47, pp. 79-91, 2004.

[20] V. A. Makarov, E. Del Rio, M. G. Bedia, M. G. Velarde, and W. Ebeling, "Central pattern generator incorporating the actuator dynamics for a hexapod robot," Transactions on Engineering, Computing and Technology, Vol.15, pp. 19-24, 2006.

Name:
Guang Lei Liu

Affiliation:
Ph.D. candidate, Department of Advanced Systems Control Engineering, Graduate School of Science and Engineering, Saga University

Address:
1-Honjomachi, Saga 840-8502, Japan

Brief Biographical History:
2005- Received M.S. degree in Advanced Systems Control Engineering, Saga University
2005- Ph.D. candidate in Advanced Systems Control Engineering, Saga University

Main Works:
• "Central Pattern Generators Based on Matsuoka Oscillators for the Locomotion of Biped Robots," Proc. of Artificial Life and Robotics, Jan. 25-27, 2007.

Membership in Academic Societies:
• The Society of Instrument and Control Engineers (SICE)

Name:
Maki K. Habib

Affiliation:
Professor, Department of Advanced Systems Control Engineering, Graduate School of Science and Engineering, Saga University

Address:
1-Honjomachi, Saga 840-8502, Japan

Brief Biographical History:
1981-1987 Lecturer, University of Technology-Baghdad
1990-1992 Selected Scientist, RIKEN-Japan
1992-1994 Senior Researcher, RISO Laboratory-Japan
1994-1995 Visiting Researcher, EPFL-Switzerland
1995-1996 Associate Professor, Malaysia University of Technology-Malaysia
1996-1999 Senior Manager for R & D and Industrial Consultation, MCRIA-Malaysia
1999-2001 Senior Research Scientist, GMD-Japan Research Centre-Japan
2001-2004 Associate Professor, Monash University-Malaysia Campus
2005-2005 Professor, Swinburne University of Technology-Malaysia Campus
2005-2006 Invited Professor, KAIST-Korea
2006-Present Visiting Professor, Saga University-Japan

Main Works:
• "Fiber Grating Based Vision System for Real Time Tracking, Monitoring and Obstacle Detection," IEEE Sensor Journal, Vol.7, No.1, pp. 105-121, Jan. 2007.
• "Map Representation for large In-door Environment, path planning and Navigation Techniques for an Autonomous mobile robot with its implementation," Int. Journal of Automation in Construction, Vol.1, No.2, pp. 155-179, 1993.

Membership in Academic Societies:
• The Institute of Electrical and Electronics Engineers (IEEE)
• International Association of Unmanned Systems (IAUS)
• Intelligent and Autonomous Systems (IAS)

Name:
Keigo Watanabe

Affiliation:
Department of Advanced Systems Control Engineering, Graduate School of Science and Engineering, Saga University

Address:
1-Honjomachi, Saga 840-8502, Japan

Brief Biographical History:
1980- Research Associate, Kyushu University
1985- Associate Professor, Shizuoka University
1990- Associate Professor, Saga University
1993- Professor, Saga University

Main Works:
• "An ART-Based Fuzzy Controller for the Adaptive Navigation of a Human-Coexistent Quadruped Robot," IEEE/ASME Trans. on Mechatronics, Vol.7, No.3, pp. 318-328, 2002.
• "Modular Fuzzy-Neuro Controller Driven by Spoken Language Commands," IEEE Trans. on Systems, Man and Cybernetics, Part B, Vol.34, No.1, pp. 293-302, 2004.
• "Neural Network-Based Kinematic Inversion of Industrial Redundant Robots Using Cooperative Fuzzy Hint for the Joint Limits Avoidance," IEEE/ASME Trans. on Mechatronics, Vol.11, No.5, pp. 593-603, 2006.

Membership in Academic Societies:
• The Japan Society of Mechanical Engineers (JSME)
• The Japan Society for Precision Engineering (JSPE)
• The Japan Society for Aeronautical and Space Sciences (JSASS)
• The Society of Instrument and Control Engineers (SICE)
• The Institute of Systems, Control and Information Engineers (ISCIE)
• The Robotics Society of Japan (RSJ)
• Japan Society for Fuzzy Theory and Intelligent Informatics (SOFT)
• The Institute of Electrical and Electronics Engineers (IEEE)

Name:
Kiyotaka Izumi

Affiliation:
Associate professor, Department of Advanced Systems Control Engineering, Graduate School of Science and Engineering, Saga University

Address:
1-Honjomachi, Saga 840-8502, Japan

Brief Biographical History:
1996- Research Associate of Saga University
2004- Associate Professor of Saga University

Main Works:
• "Evolutionary Strategy Using Statistical Information and Its Application to Mobile Robot Control," J.of Advanced Compuational Intelligence, Vol.3, No.2, pp. 75-81, 1999.
• "Obstacle Avoidance for Quadruped Robots Using a Neural Network," Int. J. of Advanced Computational Intelligence and Intelligent Informatics, Vol.7, No.2, pp. 115-123, 2003.
• "Cost Function Analysis of Optimizing Fuzzy Energy Regions in the Control of Underactuated Manipulators," Artificial Life and Robotics, Vol.10, No.2, pp. 171-175, 2006.

Membership in Academic Societies:
• Japan Society for Fuzzy Theory and Intelligent Informatics (SOFT)
• The Society of Instrument and Control Engineers (SICE)
• The Japan Society of Mechanical Engineers (JSME)
• The Robotics Society of Japan (RSJ)
• The Institute of Electronics, Information and Communication Engineers (IEICE)
• The Institute of Electrical and Electronics Engineers (IEEE)